Acta Pharm. 58 (2008) 61–74
10.2478/v10007-007-0045-1

Original research paper

Mannan-coated gelatin nanoparticles for sustained and targeted delivery of didanosine: *In vitro* and *in vivo* evaluation

AMANDEEP KAUR
SUBHEET JAIN*
ASHOK K. TIWARY

Department of Pharmaceutical Sciences and Drug Research Punjabi University, Patiala (Punjab) 147 002, India

Macrophages of the reticuloendothelial system and brain act as major reservoir for HIV because of their long term survival after HIV infection and ability to spread virus particles to bystander CD4 positive lymphocyte cells. The objective of the present study was to investigate mannan-coated nanoparticles for macrophage targeting of didanosine. Different didanosine loaded nanoparticles were prepared using the double desolvation technique and were characterized *in vitro*, *ex vivo* and *in vivo*. Results of the *ex vivo* cellular uptake study indicated 5--fold higher uptake of didanosine from the mannan-coated nanoparticles formulation (62.5 ± 5.4%) by the macrophages in comparison with didanosine solution in phosphate buffer saline (PBS, pH 7.4) (12.1 ± 2.3%). The better cellular uptake from the nanoparticles formulation was further confirmed by fluorescence microscopy using hydrophilic 6-carboxyfluorescein as a marker. Results of the quantitative biodistribution study showed 1.7, 12.6 and 12.4 times higher localization of didanosine in the spleen, lymph nodes and brain, respectively, after administration of mannan-coated nanoparticles compared to that after injection of didanosine solution in PBS (pH 7.4). Results of the present study showed that the mannan-coated nanoparticles targeted didanosine to the macrophage by mannosyl receptor mediated endocytosis.

Keywords: macrophage, targeting, didanosine, anti-HIV, mannan, receptor mediated endocytosis

Accepted February 5, 2008

Macrophages represent a key target of Human Immunodeficiency Virus (HIV) in addition to CD4 positive lymphocyte cells (CD4+). Macrophages act as a major reservoir for HIV because of their long-term survival after HIV infection and their ability to spread virus to bystander CD4+ cells (1). In organs such as brain and reticuloendothelial

* Correspondence, e-mail: subheetjain@rediffmail.com

system (RES), which is the major reservoir, HIV is located primarily in macrophages. In addition, lymph nodes play an important role in the propagation of HIV infection because replication of HIV virus at all stages of the acquired immunodeficiency syndrome (AIDS) takes place in the lymphoid tissue macrophages. Altered cellular function in the macrophages may contribute to the development and clinical progression of AIDS (2). In addition, cytokine secretion may lead to a generation of secondary events, which are likely to cause the washing syndrome, neurological manifestations of disease and change in the T helper cell response from Type 1 to Type 2. In the case of AIDS, for instance, the RES macrophage represents one of the most important therapeutic targets. This suggested the need to develop a dosage form that selectively delivers the drug to macrophages and inhibits HIV replication.

Several reports are available regarding the use of carrier systems like liposomes (3), microspheres (4) and nanoparticles (5) for macrophage targeting. Compared to other carrier systems, engineered nanoparticles are known to have better accumulation in macrophage rich organs, *e.g.*, liver, spleen, and brain due to their preferential phagocytosis (6). It is well known that brain acts as a major reservoir organ for HIV. Engineered nanoparticles have better potential to cross the blood brain barrier and deliver the drug selectively to brain macrophages (7). Therefore, engineered nanoparticles represent an interesting carrier system for the targeted delivery of antiviral agents to macrophages in an attempt to reduce the required dose, minimize toxicity, minimize dose dependent side effects, sustain the drug release and selectively deliver the drug to infected cells.

It is well known that macrophages internalize particulate carriers by the process of endocytosis. Macrophages possess various surface receptors such as Fc, mannosyl, lectin and galactosyl (8). These receptors help them in the process of recognition and endocytosis of a particulate carrier. Due to this fact, carriers containing ligands such as mannosyl, immunoglobulin, fibronectin and galactosyl are better phagocytosed by macrophages than carriers without such ligands (9).

In the present study, gelatin was selected as the polymer for preparing nanoparticles because it is biocompatible and biodegradable (10). Nanoparticles as a carrier system have distinct advantages of better accumulation in macrophage rich organs and possess the ability to cross the blood brain barrier easily compared to other carrier systems (7). Some other advantages of nanoparticles include better *in vivo* stability, ease of sterilization, ease of scale-up and prevention of contamination with pyrogens during manufacturing.

Didanosine is a widely used anti-HIV drug. However, its oral therapy is associated with poor gastrointestinal (GI) tolerability, narrow therapeutic index, several dose dependent side effects, *e.g.*, peripheral neuropathy, lactic acidosis and pancreatitis (11). In addition, oral administration of didanosine suffers from poor GI stability at pH < 3.0, first pass metabolism and variable absorption leading to poor bioavailability of 35–40% (12). This problem, together with the need for frequent dosing, low plasma protein binding (< 5%), brief plasma elimination half-life (30 min to 4 h) points to the need to develop a suitable alternative dosage form of didanosine. In the present study, an attempt has been made to formulate sustained and targeted release nanoparticles of didanosine using gelatin as polymer and mannan-coating to further enhance its macrophage uptake and its distribution in organs that act as major reservoirs of HIV.

EXPERIMENTAL

Materials

Didanosine was received as a gift sample from Cipla Ltd., India. Gelatin type A (bloom 100), mannan and 6-carboxyfluorescein (6-CF) were purchased from Sigma Chemicals, USA. Hard paraffin, wax and soft paraffin were purchased from Loba Chemie, India. Xylene, acetonitrile, diethyl ether and methanol were purchased from Ranbaxy Fine Chemicals Ltd., India.

Preparation of nanoparticles

Nanoparticles using type A gelatin as polymer were prepared using the double desolvation method described by Coester *et al.* (13) with slight modifications. Type A gelatin was dissolved in water by constant heating at 40 ± 1 °C to prepare 0.1 to 0.8% (*m/V*) solution. Acetone was added to the gelatin solution (25 mL) as a desolvating agent to precipitate the high molecular mass (HMM) gelatin. The supernatant was discarded and the HMM gelatin was redissolved by adding 25 mL distilled water and stirring at 600 rpm under constant heating at 40 ± 1 °C. An aqueous solution of the drug (0.02 to 0.24%, *m/V*) or fluorescence marker was added to the upper phase and the pH of the solution was adjusted to 4.0 with 0.1 mol L^{-1} HCl. The gelatin was then desolvated again by dropwise addition of acetone under constant stirring (1800 rpm) for 30 min. The formed gelatin nanoparticles were crosslinked with aqueous glutaraldehyde solution (8%, *V/V*) at room temperature for 10 min. The nanoparticles prepared were then sonicated (5 to 20 min). The particles were then purified by centrifugation at 10,000 rpm for 20 min and the resulting nanoparticles were stored at 2–8 °C.

Mannan-coating of nanoparticles

Mannan-coating of the optimized nanoparticles formulation (N-C3) was carried out using the incubation method (5). Coating solutions were prepared by dissolving mannan (1.0%, *m/V*) in hot water. Coating was done by depositing these coating solutions on the surface of nanoparticles by mixing 1.0 mL of the preformed nanoparticle suspension with mannan solution and stirring this mixture overnight at room temperature. Free mannan was removed by passing through a Sephadex G-75 column (14 × 65 mm).

Nanoparticle characterization

Shape. – The morphology of plain and mannan-coated nanoparticles was determined by transmission electron microscopic studies on a Philips EM268D instrument (Philips, The Netherlands) at a voltage of 80 kV using the desired magnification. A thin film of nanoparticle sample was mounted on a carbon-coated grid. The grid was dried in a desiccator at room temperature (25 ± 1 °C) before loading onto the microscope.

Size and zeta potential. – The particle size and size distribution of the nanoparticle was determined by the laser diffraction method (Malvern, Zeta master, ZEM5002, Malvern, UK). The nanoparticle suspension (1.0 mL) was dispersed in 4.0 mL water. Measu-

rements were carried out at 25 ± 1 °C by scattering light at 90°. The mean particle size and size distribution were determined. The zeta potential of the formulation was determined using the same instrument.

Entrapment efficiency. – Entrapment efficiency of different batches of nanoparticles was determined by the method proposed by Vandervoort and Ludwig (14). The amount of didanosine entrapped was determined by incubating the nanoparticle suspension (1.0 mL) in 5.0 mL phosphate buffer saline (PBS, 7.4) for two hours at 800 rpm at 25 ± 0.5 °C in a shaker incubator. The amount of unbound drug was determined spectrophotometrically (Beckman, DU-64OB, USA) at 250 nm in the supernatant obtained after separation of nanoparticles by centrifugation at 13000 spm for 30 min.

Differential scanning calorimetry (DSC). – Physical mixtures of gelatin and drug and drug-loaded nanoparticles were subjected to DSC analysis. Samples were accurately weighed into DSC aluminum pans. The samples were then heated at a rate of 5 °C min^{-1} from 25 to 300 °C (Mettler, Toledo Star System, 821E, Switzerland).

In vitro *drug release.* – *In vitro* drug release from drug-loaded plain and mannan-coated nanoparticles was evaluated using the equilibrium dialysis technique at 37 ± 1 °C. Briefly, 2 mL of nanoparticle dispersion were put in the dialysis bag (Himedia, MWCO, molecular mass cut off 12000–14000, pore size 2.4 nm) and were dialyzed against 100 mL of PBS 7.4 at a rotation speed of 50 rpm. At predetermined time intervals, 1.0 mL samples were withdrawn from sampling port, filtered through 0.45-μm membrane filter and the drug content was determined spectrophotometrically. The receptor phase volume was replenished with an equal volume of fresh PBS maintained at 37 ± 1 °C.

Ex vivo *cellular uptake studies.* – The *ex vivo* cellular uptake of mannan-coated nanoparticles (N-C3-M), plain nanoparticle (N-C3) and PBS solution of the drug was carried out by incubating 1 mL formulation with 2 mL of heparinized human blood at 37 ± 1 °C. After 2 h of incubation, the blood was added to agarose and fucose (2%) dispersion media and centrifuged at 10000 rpm for 10 min to separate monocytes/neutrophils and macrophages. The smears were prepared on microscopic slides and dried. They were then stained with Leishmann's stain, washed with distilled water and allowed to dry (15). The slides were then examined under an optical microscope. Shape and morphology of monocytes and macrophages were observed and compared with the microscopic examination of blood incubated with the drug solution in PBS under the same set of conditions. Phagocytosis (%) was determined by counting the number of macrophages that had undergone phagocytosis out of 100 cells observed at 100x magnification. At the same time, 150 μL of cell suspension was taken and an equal volume of 10% trichloroacetic acid solution in water was added and mixed for 2 min. The mixture was then centrifuged at 3000 rpm for 10 min and a supernatant was filtered through a 0.45-μm membrane filter and the drug content was determined by the HPLC assay (16).

HPLC assay. – Didanosine in biological fluids was estimated by the HPLC method as reported by Courtney *et al.* (16). Acetonitrile (5%) in 50 mmol L^{-1} ammonium phosphate buffer (pH 6.7) was used as mobile phase and was delivered at 1.0 mL min^{-1}. The injected fluid (20 μL) was eluted in C8 column at room temperature and didanosine was monitored at 250 nm using a UV detector (Waters, USA). The calibration curve with in a concentration range from 0.05 to 10.0 μg mL^{-1} was used to measure the didanosine con-

centration. The relative standard deviation around the calibration line ranged from 1.0 to 6.0% and the squared correlation coefficient was over 0.9915.

Fluorescence microscopy. – Rats (Sprague Dawley strain), 6 to 8 weeks old, weighing 100–150 g, were divided into four groups of three rats each. First group received a subcutaneous injection (*s.c.*) of 1.0 mL of 0.16% (*m/V*) solution of fluorescence marker 6-CF in PBS (pH 7.4) in the dorsal part of hind paw. Second group received 1.0 mL of 0.16% (*m/V*) solution of marker 6-CF orally. Third and fourth groups received subcutaneous injection of 1.0 mL of the optimized plain nanoparticle formulation (N-C3) and mannan-coated nanoparticle formulation (N-C3-M) loaded with 6-CF (0.16%, *m/V*), respectively, in the dorsal part of hind paw. Rats were sacrificed after 12 h of administration and selected tissues (spleen, liver and lymph nodes) were excised, cut into small pieces and fixed using the conventional method (17). Paraffin blocks were made, 5-μm thick sections were cut using a microtome (Erma Optical Works, Japan) and examined under a fluorescence microscope (Leica, DMRBE, Germany).

All investigations were performed after approval by the Institutional ethical committee and in accordance with the disciplinary principles and guidelines of CPCSEA (Committee for the purpose of control and supervision of experiments on animals).

Biodistribution studies. – The protocol used for the biodistribution study was similar to those described for the fluorescence microscopy study. Sprague Dawley rats (6 to 8 weeks old, weighing 100–150 g) were divided into four groups of three rats each. First group received a subcutaneous injection of 1.0 mL of 0.16% (*m/V*) solution of didanosine in PBS (pH 7.4) in the dorsal part of hind paw. Second and third groups received a subcutaneous injection of 1.0 mL of the plain nanoparticle formulation (N-C3) and mannan-coated nanoparticle formulation (N-C3-M), both loaded with didanosine (0.16%, *m/V*), respectively, in the dorsal part of hind paw. Fourth group received 1.0 mL of 0.16% (*m/V*) solution of didanosine in PBS orally. The dose of didanosine selected for animal study was 20.0 mg kg^{-1} as reported by Kaul *et al.* (18). Rats were sacrificed after 12 h of administration and blood was collected by cardiac puncture. At the same time, selected tissues (spleen, liver, kidney, lymph nodes and brain) were excised, isolated, dried and weighed. Blood was collected from cardiac puncture in a centrifuge tube at predetermined time intervals and centrifuged at 2000 rpm for 10 minutes. Supernatant was collected and acetonitrile was added to precipitate the proteins. The precipitated proteins were settled by centrifugation at 2000 rpm for 15 min and the supernatant was collected. One mL of collected supernatant was filtered through a 0.45-μm filter into a 10-mL volumetric flask. Volume was made up with the mobile phase (5% acetonitrile in 50 mmol L^{-1} ammonium phosphate buffer) and the drug concentration was determined by the HPLC assay.

Various organs (liver, spleen, kidney, lymph nodes and brain) were homogenized after drying with 2 mL of PBS (7.4) using a tissue homogenizer. To the tissue homogenate, an equal volume of 10% (*V/V*) trichloroacetic acid (in water) was added and vortexed for 30 s to precipitate tissue proteins. After precipitation of proteins, the drug was extracted by adding 10 mL of acetonitrile, followed by equilibration for 30 min at room temperature (19). The tubes were then centrifuged for 30 min at 3000 rpm. After filtration through membrane filter, the filtrate was assayed for didanosine by the HPLC assay as described earlier.

Statistical analysis

Statistical analysis of data was performed using the analysis of variance (ANOVA).

RESULTS AND DISCUSSION

Nanoparticle formulations were prepared using the double desolvation technique as described by Coester *et al.* (13) because the nanoparticles prepared by this method are reported to be spherical and to exhibit small particle size, low polydispersity index and high yield. pH selected for coacervation was 4.0 because of the poor stability of the drug at pH < 3.0 (20). Stability study of the drug during nanoparticle preparation, as determined by HPLC, did not show significant degradation Initially, gelatin nanoparticles were prepared using different drug concentrations (N-A1 to N-A5 containing 0.02 to 0.24%, *m/V*, didanosine), different polymer concentrations (N-B1 to N-B4 containing 0.1 to 0.8%, *m/V*, of gelatin) and using different sonication times (N-C1 to N-C4, 5 to 20 min) (Table I). All these formulations were optimized on the basis of shape, size, entrapment efficiency and *in vitro* drug release (Table II).

Table I. Composition of different nanoparticle formulations

Formulation code	Drug (%, *m/V*)	Gelatin (%, *m/V*)	Sonication time (min)	Mannan (%, *m/V*)
Optimization of drug load				
N-A1	0.02	0.2	5	–
N-A2	0.04	0.2	5	–
N-A3	0.08	0.2	5	–
N-A4	0.16	0.2	5	–
N-A5	0.24	0.2	5	–
Optimization of gelatin conc.				
N-B1	0.16	0.1	5	–
N-B2	–	0.2	5	-
N-B3	–	0.4	5	–
N-B4	–	0.8	5	–
Optimization of sonication time				
N-C1	0.16	0.8	5	–
N-C2	0.16	0.8	10	–
N-C3	0.16	0.8	15	–
N-C4	0.16	0.8	20	–
Mannan-coating				
N-C3-M	0.16	0.8	15	1.0

Table II. In vitro *characterization of different nanoparticle formulations*[a]

Formulation code	Morphology	Entrapment efficiency (%)	Particle size (nm)	Drug release (%) after 24 h
N-A1	Aggregate	68.4 ± 1.4	210 ± 12	49.0 ± 3.1
N-A2	Aggregate	68.6 ± 2.2	213 ± 10	56.5 ± 3.5
N-A3	Aggregate	70.2 ± 2.3	211 ± 13	61.9 ± 3.7
N-A4	Aggregate	72.4 ± 2.0	218 ± 15	69.0 ± 2.3
N-A5	Aggregate with appearance of drug crystal	69.2 ± 2.4	215 ± 10	86.9 ± 4.5
N-B1	Aggregate	64.3 ± 2.3	214 ± 15	75.0 ± 3.1
N-B2	Aggregate	72.4 ± 2.0	218 ± 15	69.0 ± 2.3
N-B3	Aggregate	71.5 ± 2.3	228 ± 14	63.9 ± 3.7
N-B4	Aggregate with smooth surface	70.8 ± 2.5	235 ± 10	61.9 ± 2.7
N-C1	Aggregate	70.7 ± 3.7	235 ± 10	63.0 ± 4.8
N-C2	Discrete with smooth surface	71.0 ± 3.6	162 ± 4.0	61.5 ± 3.4
N-C3[b]	Discrete with perfectly smooth surface	71.2 ± 3.5	120 ± 12	58.8 ± 2.9
N-C4	Discrete with perfectly smooth surface	72.5 ± 2.1	94 ± 10	57.7 ± 3.2

[a] Data are represented as mean ± SD, $n = 3$.
[b] Optimized formulation.

Better uptake in the lymphatic system macrophages with the carrier system having the size 100 to 150 nm is reported (3). Hence, to obtain nanoparticles in the desired size range, the formulation was sonicated for 5, 10, 15 or 20 min. Dynamic light scattering revealed that an increase in sonication time from 5 to 15 min led to significant decrease in particle size from 235 ± 10 nm to 120 ± 12 nm for batch N-C3 ($p < 0.05$) (Table II). Hence, 15 min was considered as the optimum sonication time for preparation of nanoparticles in a size range of 100–150 nm.

Mannan-coating of nanoparticles was undertaken with a view to increase their uptake by the macrophage through receptor-mediated endocytosis (6). Optimum batch of gelatin nanoparticles (N-C3) was coated with mannan (1.0%, *m/V*). Batch N-C3 was selected as the optimum batch because it exhibited high entrapment efficiency (71.2 ± 3.5%), sustained release characteristic (58.8 ± 2.9% after 24 h) and desired particle size (120 ± 12 nm). The coating of nanoparticles was confirmed by visualizing the nanoparticles using transmission electron microscopy (Fig. 1) as well as by measuring the zeta potential and particle size of coated formulation (Table III). Nanoparticles were found to be spherical in shape and exhibited a significantly thick and smooth surface after subsequent coating with mannan and a significant increase ($p < 0.05$) in the size of the particles from 120 ± 12 nm to 140 ± 19 nm (batch N-C3-M).

Figs. 2a-b show the DSC profiles of the physical admixture of didanosine and gelatin and gelatin nanoparticles. DSC thermogram of the physical admixture showed two

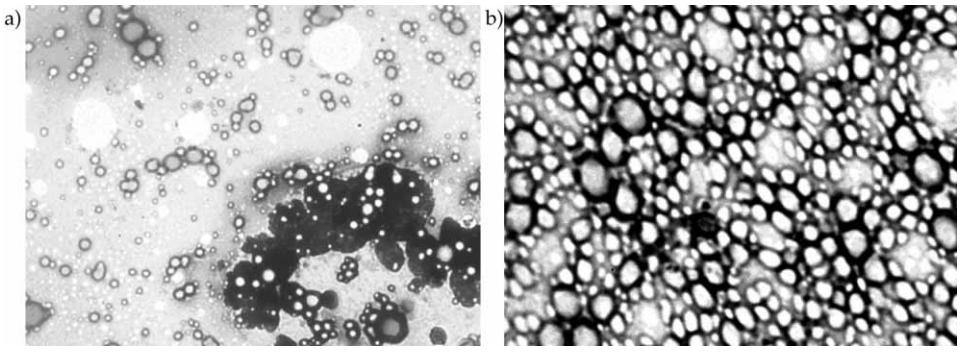

Fig. 1. Transmission electron microscopy photomicrograph of: a) plain nanoparticles (N-C3) and mannan-coated nanoparticles formulation (N-C3-M) (both 15000x magnification). Error bar = 50 nm.

endothermic peaks at 102.5 °C and 182.0 °C. Endothermic peak at 182 °C represents the didanosine melting point near 180 °C and another peak near 100 °C is from gelatin (21). The results obtained are in good agreement with those reported by Sanchez-Lafuente *et al.* (22). They also found the endothermic peak of didanosine at around 180 °C. In contrast, the profile of the lyophilized powder of gelatin nanoparticles showed a single peak around 200 °C (Fig. 2b) suggesting the occurrence of unique molecular interactions in these nanoparticles. Taken together, these DSC profiles of gelatin nanoparticles demonstrate that the gelatin nanoparticles, which were engineered from the desolvation process comprising gelatin and didanosine, were not a simple physical admixture of the two components. Cui *et al.* (5) also found that cationic gelatin nanoparticles consisting of emulsifying wax and cetyl trimethyl ammonium bromide (CTAB) showed single peak in the thermogram but when tested in physical admixture, different peaks appeared for each component in the thermogram.

Fig. 3 compares the *in vitro* drug release profile of didanosine from mannan-coated nanoparticles, plain nanoparticles and drug suspension. Drug was released from plain

Table III. Characterization of plain and mannan-coated nanoparticles

Parameter	Plain nanoparticles (N-C3)	Mannan-coated nanoparticles (N-C3-M)
Particle size (nm)	120 ± 12	140 ± 19
Entrapment efficiency (%)	71.2 ± 3.5	79.5 ± 4.7
Zeta potential (ζ, mV)	18.6 ± 2.1	7.2 ± 1.8
Surface morphology	Smooth	Perfectly smooth
Drug release after 24 h (%)	58.8 ± 2.9	42.5 ± 1.7

[a] Data are represented as mean ± SD, $n = 3$.

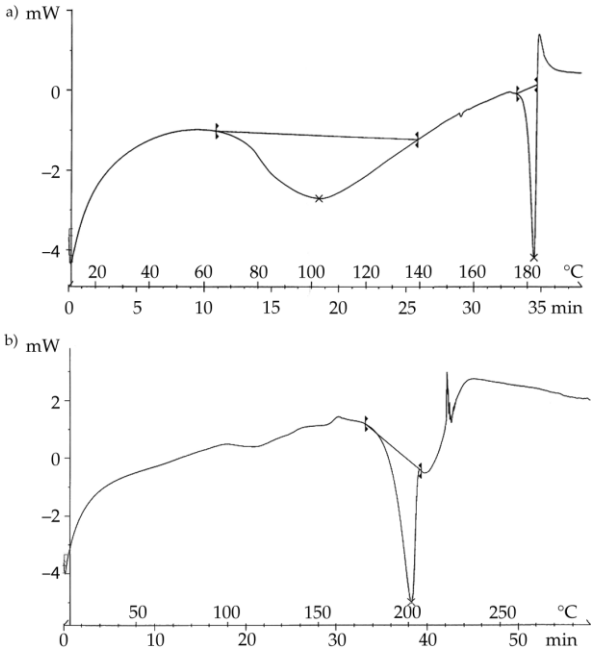

Fig. 2. DSC thermogram of: a) physical admixture of didanosine and gelatin and b) optimized nanoparticles formulation (N-C3).

nanoparticles completely within 2 h (98.8 ± 4.5%) compared to the gelatin nanoparticles (N-C3), which showed only 58.8 ± 2.9% drug release over 24 h. Coating of nanoparticles with mannan further retarded the drug release (42.5 ± 1.7% over 24 h). The concentration of gelatin employed for the preparation of nanoparticles had a significant effect on

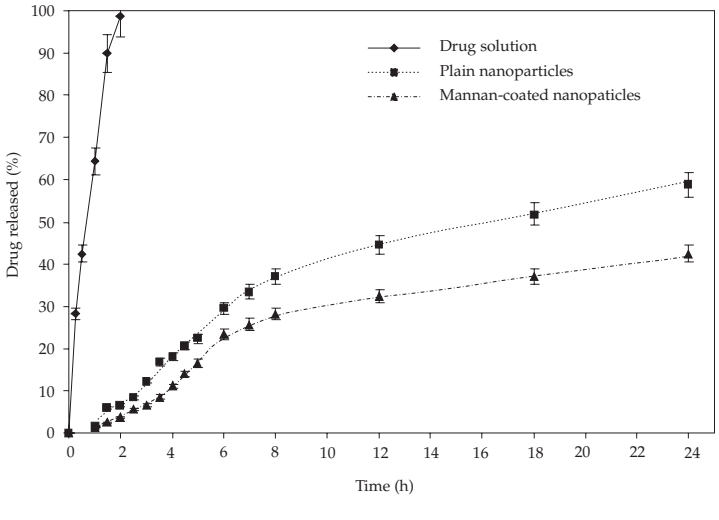

Fig. 3. *In vitro* drug release of didanosine from plain nanoparticles (N-C3), mannan-coated nanoparticle (N-C3-M) and dissolved drug (mean ± SD, n = 3).

the release rate. Increasing the gelatin concentration from 0.1 to 0.8%, *m/V*, significantly ($p < 0.05$) decreased the release rate from 75.0 ± 3.1% (N-B1) to 61.9 ± 2.7% (N-B4) over 24 h. This may be due to the increase in the diffusion bilayer size as a result of the increase in the concentration of gelatin, which sustained the release of didanosine from the nanoparticles.

Table IV shows the morphological characteristics of Leishmann's stained macrophages after incubation with PBS (pH 7.4) solution of didanosine, didanosine-loaded plain and mannan-coated nanoparticles. Microscopic visualization of the macrophages incubated with mannan-coated optimized nanoparticle formulation showed a prominent effect on the morphology of macrophages (Table IV). After incubation with mannan-coated nanoparticles, these cells became swollen due to the uptake of nanoparticles and the macrophage nucleus was observed to be nearly separated from the remaining cellular contents. Further, complete lysis of macrophage membrane was evident with some of the cells. However, after incubation with the drug solution, the effect on cell nucleus was not prominent. Plain nanoparticles show effects similar to mannan-coated nanoparticles but to a lesser extent. Coating of nanoparticles with mannan further increased the cellular uptake of nanoparticles (N-C3-M) as evident by higher staining intensity and complete lysis within 2 h of incubation. The results of phagocytosis measurement also displayed a greater uptake of nanoparticle formulations compared to the drug solution. Mannan-coated nanoparticles showed 88.7 ± 6.2% phagocytosis (N-C3-M) after 2 h of incubation, whereas plain nanoparticles (N-C3) and drug solution showed only 51.2 ± 4.6 and 21.7 ± 2.8%, respectively (Table IV).

Table IV. Observation of ex vivo *cellular uptake studies*

Parameter	Drug solution in PBS	Plain nanoparticles	Mannan-coated nanoparticles
Adsorption	+	+	+++
Uptake	+	+	+++
Swelling	–	++	+++
Lysis	–	++	+++
Phagocytosis (%)	21.7 ± 2.8	51.2 ± 4.6	88.7 ± 6.2

— – none; + – slight; ++ – moderate; +++ – good

The better cellular uptake of mannan-coated nanoparticles might be due to the presence of mannosyl receptor predominantly on the macrophage cell surface, which is used by the cells for endocytosis and phagocytosis (5, 23). Mannosyl receptor recognizes mannan on cell walls of the infectious agent in the body (24). Upon binding, there is aggregation and receptor mediated endocytosis. This causes mannan-coated nanoparticles to be phagocytized by the macrophage at a faster rate. The quantitative cellular uptake measurement studies showed after 2 h of incubation five times higher uptake of didanosine from mannan-coated nanoparticles (62.5 ± 5.4%) and its 3 times higher uptake from plain nanoparticles (37.2 ± 4.1%) compared to drug solution (12.1 ± 2.3%). Results of the cellular uptake study were well correlated with those reported by Cui *et al.* (5) for the

uptake of mannan-coated gelatin nanoparticles in a mannose receptor positive (MR+) mouse macrophage cell line.

The better cellular uptake of the nanoparticle formulation was further confirmed by fluorescence microscopy. Marker selected for the present study was 6-CF because it has a similar hydrophilic nature to didanosine (17). Fluorescence photomicrographs (not shown) reveal better qualitative uptake and localization of fluorescence marker loaded plain nanoparticles and mannan-coated nanoparticles in brain, spleen and lymph nodes as compared to its solution. This supports the results of the *ex vivo* cellular uptake study. Significantly higher concentration of the fluorescence marker, shown by higher fluorescence intensity, was observed after 12 h of administration in brain, spleen and lymph nodes. No fluorescent signal was observed in the control group and a relatively weak signal was observed in case of animals treated with marker-loaded plain nanoparticles.

Biodistribution pattern of the free drug, plain and mannan-coated nanoparticles into different organs was measured and the results are shown in Fig. 4**.** The organ distribution pattern, plasma concentration of didanosine in case of different formulations and free drug indicate the superiority of the nanoparticulate system in increasing the accumulation of didanosine in various target organs, specially in spleen, lymph nodes and brain and its lowering in lung and kidney. Mannan-coated nanoparticles showed 12-fold higher lymphatic distribution of the drug in comparison with drug solution in PBS. The reason for better lymphatic uptake of mannan-coated nanoparticles is their preferential phagocytosis by macrophages and localization in lymph nodes. After the *s.c.* injection of nanoparticles into the dorsal side of the the foot, nanoparticles are efficiently absorbed *via* lymphatic capillaries and localized in the lymph nodes. It has been suggested that phagocytosis by macrophages is one of the major mechanisms of uptake of colloidal particles in lymph nodes (25).

Conventional formulations like tablets, capsules and suspensions are not able to deliver the drug to brain due to the nature of the blood-brain barrier (BBB). Fig. 4 compares the brain concentration of didanosine after its administration in the form of drug so-

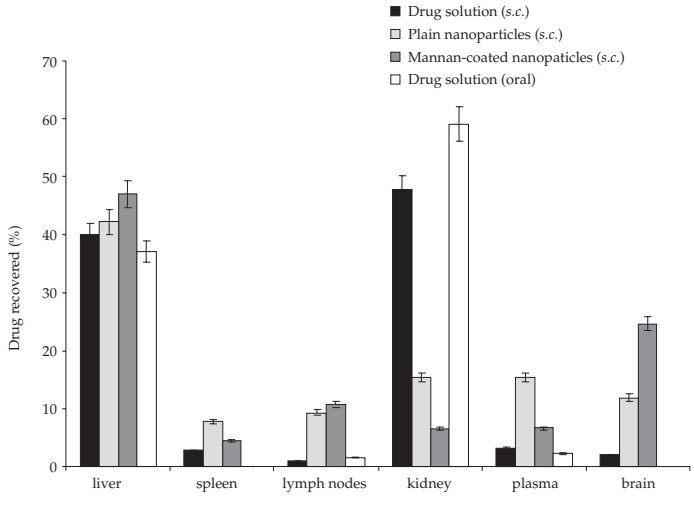

Fig. 4. Tissue distribution of didanosine (after 12 h of application) administered as mannan--coated nanoparticles (N-C3-M), plain nanoparticles (N-C3) and drug solution (mean ± SD, n = 3).

lution, plain nanoparticles and mannan-coated nanoparticles. The results showed 12.4- and 6.0- fold higher accumulation of didanosine in brain when administered through mannan-coated nanoparticles and plain nanoparticles compared to drug solution. This was due to the presence of mannosyl receptors on macrophage cells of the brain mononuclear phagocytic system as well as the inherent ability of nanoparticles to cross the BBB by opening the tight junction between endothelial cells. This would lead to increased retention of nanoparticles in the brain capillaries combined with absorption to capillary walls by receptor mediated endocytosis (6, 7). Didanosine is a hydrophilic drug and its ability to cross the BBB is very low (11); however, mannan-coated nanoparticles represent a better approach for enhanced delivery of didanosine to brain.

The reason for better accumulation of mannan-coated gelatin nanoparticles is their preferential macrophage uptake by RES organs, lymph nodes and brain. After administration, nanoparticles are selectively taken up by the macrophage rich organs by receptor-mediated endocytosis due to the presence of mannosyl receptor on the cell surface. After reaching inside the cell, these nanoparticles are degraded by lysosomes and entrapped didanosine is released. This released didanosine will be selectively delivered to HIV, which mainly resides in the macrophage and prevent its replication. The main rate limiting step in this process is the stable adsorption of nanoparticles on the cell surface (8, 9). Due to the presence of mannosyl receptor on the macrophage cell surface, these mannan-coated nanoparticles have a high probability of stable absorption on cell surface followed by endocytosis, as evident from the *ex vivo* cellular uptake study. In contrast, free didanosine in solution is very poorly adsorbed on macrophage surface, which results in a smaller amount of drug reaching the internal compartment of macrophages.

CONCLUSIONS

Administration of mannan-coated gelatin nanoparticles resulted in a significantly higher concentration of didanosine in spleen, lymph nodes and brain. These nanoparticles sustained the release of didanosine and may be used to reduce the frequency of administration and dose-dependent side-effects, reducing the chances of dose dumping and increasing the patient compliance.

Acknowledgements. – Authors are grateful to M/s Cipla Ltd., India, for providing didanosine as a gift sample. Director, Electron Microscopy Section, AIIMS, New Delhi, India, is acknowledged for providing the facilities for electron microscopy. The authors are also grateful to the Head, Department of Zoology, Punjabi University, Patiala, for providing the necessary facilities for optical and fluorescence microscopy.

REFERENCES

1. M. S. Meltzer, D. R. Skillman, P. J. Gomatos, D. C. Kalter and H. C. Gendelman, Role of mononuclear phagocytosis in the pathogenesis of human immunodeficiency virus infection, *Annu. Rev. Immunol.* **8** (1990)169–194; DOI: 10.1146/annurev.iy.08.040190.001125.
2. S. Aquaro, R. Calio, J. Balzarini, M. C. Bellocchi, E. Garaci and C. F. Perno, Macrophages and HIV infection: therapeutical approaches toward this strategic virus reservoir, *Antiviral Res.* **55** (2002) 209–225; DOI: 10.1016/S0166-3542(02)00052-9.

3. C. Oussoren, M. Magnani, A. Fraternale, A. Casabianca, L. Chiarantini, R. Ingebrigsten, W. J. M. Underberg and G. Strome, Liposomes as carrier of the antiretroviral agent dideoxycytidine-5'--triphosphate, *Int. J. Pharm.* **180** (1999) 261–270; DOI: 10.1016/S0378-5173(99)00016-2.
4. V. Schafer, H. V. Briesen, H. Rubsamen-Waigmann, A. M. Steffan, C. Royer and J. Kreuter, Phagocytosis and degradation of human serum albumin microspheres and nanoparticles in human macrophages, *J. Microencaps.* **11** (1994) 261–269; DOI: 10.3109/02652049409040455.
5. Z. Cui, C. H. Hsu and R. J. Mumper, Physical characterization and macrophage cell uptake of mannan-coated nanoparticles, *Drug Dev. Ind. Pharm.* **29** (2003) 689–700; DOI: 10.1081/DDC-120021318.
6. F. Ahsan, I. P. Rivas, M. A. Khan and A. I. T. Suarez, Targeting of macrophage: role of physicochemical properties of particulate carriers-liposomes and microsphere on the phagocytosis by macrophages, *J. Control. Rel.* **79** (2002) 29–40; DOI: 10.1016/S0168-3659(01)00549-1.
7. J. Kreuter, Nanoparticulate system for brain delivery of drugs, *Adv. Drug Deliv. Rev.* **47** (2001) 65–81; DOI: 10.1016/S0169-409X(00)00122-8.
8. M. S. Wadhwa and K. G. Rice, Receptor mediated glycotargeting, *J. Drug Target.* **11** (2003) 255–268; DOI: 10.1080/10611860310001636557.
9. J. Shao and J. K. H. Ma, Characterization of mannosylphospholipid liposome system for drug targeting to alveolar macrophages, *J. Drug Deliv. Target. Ther. Agents* **4** (1997) 43–48.
10. Y. Gabr, N. Assem, A. Micheal and L. Fahmy, Evaluation studies on oxypolygelatin and degraded gelatin as plasma volume expanders, *Arzneimittelforschung* **46** (1996) 763–766.
11. R. Yarchoan, H. Mitsuya, R. V. Thomas, J. M. Pluda, N. R. Hartman and C. F. Perno, In vivo activity against HIV and favorable toxicity profile of 2'3'-dideoxyinosine, *Science* **245** (1989) 412–417.
12. T. P. Cooley, M. L. Kunches, C. A. Saunders, C. J. Perkins, S. L. Kelley, C. McLaren, R. P. McCaffrey and H. A Liebman, Treatment of AIDS and AIDS related complex with 2'3'-dideoxyinosine given once daily, *Rev. Infect. Dis.* **12** (1990) S552–S560.
13. C. J. Coester, K. Langer, H. Von Briesen and J. Kreuter, Gelatin nanoparticles by two step desolvation – A new preparation method, surface modification and cell uptake, *J. Microencaps.* **17** (2000) 187–193; DOI: 10.1080/026520400288427.
14. J. Vandervoort and A. Ludwig, Preparation and evaluation of drug-loaded gelatin nanoparticles for topical ophthalmic use, *Eur. J. Pharm. Biopharm.* **57** (2004) 251–261; DOI: 10.1016/S0939-6411(03)00187-5.
15. E. Rebasamen, W. Goldinger, W. Scheirer, O. W. Merten and G. E. Palfe, *Development in Biological Standardization*, in *Advances in Animal Cell Technology and Cell Engineering: Evaluation and Exploitation* (Eds. R. Spier and W. Hennessen), Vol. 66, ESACT, Basel 1987, pp. 557–583.
16. V. F. Courtney, R. C. Brundage, R. P. Remmel, L. M. Page, D. Weller, N. R. Calles, C. Simon and M. W. Kline, Pharmacologic characteristic of indinavir, didanosine and stavudine in human immunodeficiency virus-infected children receiving combination therapy, *Antimicrob. Agents Chemother.* **44** (2000) 1029–1034.
17. S. Jain, R. Sapre, A. K. Tiwary and N. K. Jain, Proultraflexible lipid vesicles for effective transdermal delivery of levonorgestrel: Development, characterization and performance evaluation, AAPS *PharmSciTech.* **6** (2005) E513–E522; DOI: 10.1208/pt060364.
18. S. Kaul, W. C. Shyu, U. A. Shukla, K. A. Dandekar and R. H. Barbhaiya, Pharmacologic characteristic of indinavir, didanosine and stavudine in human immunodeficiency Virus-Infected children receiving combination therapy, *Drug Metab. Dispos.* **21** (1993) 447–453.
19. E. Mukherji, N. J. Millenbaugh and J. L. S. Au, Percutaneous absorption of 2', 3'-dideoxyinosine in rats, *Pharm. Res.* **11** (1994) 809–815.
20. O. Bekers, J. H. Beijnen, M. J. T. Klein Tank, D. M. Burger, P. I. Meenhorst, A. J. P. F. Lombarts and W. J. M. Underberg, 2',3'-dideoxyinosine (ddI): Its chemical stability and cyclodextrin com-

plexation in aqueous media, *J. Pharm. Biomed. Anal.* **11** (1993) 489–493; DOI: 10.1016/0731-7085 (93)80162-T.

21. P. T. Tayade and R. D. Kale, Encapsulation of water-insoluble drug by a cross-linking technique: Effect of process and formulation variables on encapsulation efficiency, particle size, and *in vitro* dissolution rate, AAPS *Pharm. Sci* **6** (2004); DOI: 10.1208/ps060112.
22. C. Sanchez-Lafuente, A. M. Rabasco, J. Alvarez-Fuentes and M. Fernandez-Arevalo, Eudragit® RS-PM and Ethocel® 100 premium: influence over the behavior of didanosine inert matrix system, *Farmaco* **57** (2002) 649–656; DOI: 10.1016/S0014-827X(02)01240-5.
23. V. Apostolopoulos and I. F. McKenzie, Role of the mannose receptor in the immune response, *Curr. Mol. Med.* **1** (2001) 469–474; DOI:10.2174/1566524013363645.
24. C. A. Hoppe and Y. C. Lee, The binding and processing of mannose-bovine serum albumin derivatives by rabbit alveolar macrophages. Effect of the sugar density, *J. Biol. Chem.* **258** (1983) 14193–14199.
25. M. Velinova, N. Read, C. Kirby and G. Gregoriadis, Morphological observation on the fate of liposomes in the regional lymph nodes after footpad injection into rats, *Biochim. Biophys. Acta* **1299** (1996) 207–215; DOI: 10.1016/0005-2760(95)00208-1.

S A Ž E T A K

Želatinske nanočestice obložene mananom za polaganu i ciljanu isporuku didanozina: *In vitro* i *in vivo* vrednovanje

AMANDEEP KAUR, SUBHEET JAIN i ASHOK K. TIWARY

Makrofagi retikuloendotelnog sustava i mozak djeluju kao glavni rezervoari za HIV zbog njihovog dugoročnog preživljavanja nakon infekcije HIV-om i sposobnosti da usmjere virusne čestice u CD4 pozitivne limfocite. Cilj rada bio je ispitati nanočestice obložene mananom za ciljanu isporuku didanozina u makrofage. Koristeći metodu dvostruke desolvatacije pripravljene su različite nanočestice s didanozinom te su zatim karakterizirane *in vitro*, *ex vivo* i *in vivo*. Rezultati *ex vivo* ispitivanja ukazuju da je unos didanozina u makrofage 5 puta veći iz nanočestica obloženih mananom (62,5 ± 5,4%) u usporedbi s otopinom didanozina u fosfatnom puferu (PBS, pH 7,4) (12,1 ± 2,3%). Bolji celularni unos iz nanočestica potvrđen je fluorescentnom mikroskopijom koristeći hidrofilni 6-karboksifluorescein kao marker. Rezultati kvantitativne biodistribucije pokazuju da je lokalizacija didanozina u slezeni, limfnim čvorovima i mozgu 1,7, 12,6, odnosno 12,4 puta veća nakon primjene nanočestica obloženih mananom nego nakon primjene otopine didanozina u PBS-u (pH 7,4). Nanočestice s mananom usmjeravaju didanozin u makrofage procesom endocitoze u kojoj posreduju receptori za manozu.

Ključne riječi: makrofag, ciljana terapija, didanozin, anti-HIV, manan, endocitoza posredovana receptorima

Department of Pharmaceutical Sciences and Drug Research, Punjabi University, Patiala (Punjab) 147 002, India